

## RED CELLS, IRON, AND ERYTHROPOIESIS

Cytoadhesion of *Plasmodium falciparum*-infected erythrocytes to chondroitin-4-sulfate is cooperative and shear enhancedHarden Rieger,<sup>1,2</sup> Hiroshi Y. Yoshikawa,<sup>2,3</sup> Katharina Quadt,<sup>1</sup> Morten A. Nielsen,<sup>4</sup> Cecilia P. Sanchez,<sup>1</sup> Ali Salanti,<sup>4</sup> Motomu Tanaka,<sup>2,5</sup> and Michael Lanzer<sup>1</sup><sup>1</sup>Department of Infectious Diseases, Parasitology, and <sup>2</sup>Institute of Physical Chemistry, Physical Chemistry of Biosystems, Heidelberg University, Heidelberg, Germany; <sup>3</sup>Department of Chemistry, Saitama University, Saitama, Japan; <sup>4</sup>Center for Medical Parasitology, University of Copenhagen, Copenhagen, Denmark; and <sup>5</sup>Institute for Integrated Cell-Material Science, Kyoto University, Kyoto, Japan

## Key Points

- Cytoadhesion of parasitized erythrocytes depends on the intermolecular distance between neighboring chondroitin-4-sulfate molecules.
- VAR2CSA is an allosteric adhesin that binds chondroitin-4-sulfate in a cooperative and shear stress-induced manner.

Infections with the human malaria parasite *Plasmodium falciparum* during pregnancy can lead to severe complications for both mother and child, resulting from the cytoadhesion of parasitized erythrocytes in the intervillous space of the placenta. Cytoadherence is conferred by the specific interaction of the parasite-encoded adhesin VAR2CSA with chondroitin-4-sulfate (CSA) present on placental proteoglycans. CSA presented elsewhere in the microvasculature does not afford VAR2CSA-mediated cytoadhesion of parasitized erythrocytes. To address the placenta-specific binding tropism, we investigated the effect of the receptor/ligand arrangement on cytoadhesion, using artificial membranes with different CSA spacing intervals. We found that cytoadhesion is strongly dependent on the CSA distance, with half-maximal adhesion occurring at a CSA distance of  $9 \pm 1$  nm at all hydrodynamic conditions. Moreover, binding to CSA was cooperative and shear stress induced. These findings suggest that the CSA density, together with allosteric effects in VAR2CSA, aid in discriminating between different CSA milieus. (*Blood*. 2015;125(2):383-391)

## Introduction

The virulence of tropical malaria is largely associated with the blood-stage cycle of the protozoan parasite *Plasmodium falciparum* and the adhesive behavior of parasitized erythrocytes, which sequester in the deep vascular bed of inner organs to avoid passage through, and destruction in, the spleen.<sup>1</sup> The pathological sequelae that develop in affected capillaries can progress to life-threatening complications and include diminished tissue perfusion, hypoxia, and systemic microvascular inflammation.<sup>1</sup>

Cytoadhesion of parasitized erythrocytes is mediated by a family of parasite-encoded immunovariant adhesins, collectively termed PfEMP1, that can interact with a broad range of host cell receptors, including CD36, intercellular adhesion molecule 1 (ICAM 1), P-selectin, and vascular cell adhesion molecule 1 (VCAM 1).<sup>1</sup> A defined PfEMP1 variant encoded by the *var2CSA* gene can further mediate attachment of parasitized erythrocytes to chondroitin-4-sulfate (CSA). CSA is thought to be a component of the proteoglycan matrix present in the intervillous space and (moderately) on the syncytiotrophoblast cell layer of the human placenta,<sup>2-5</sup> although one study has suggested that placental CSA is of fetal origin and is in contact with maternal blood only in the advanced and chronically infected placenta after syncytiotrophoblast denudation.<sup>6</sup> According to this latter study, initial steps of placental cytoadhesion might

involve Lewis antigens and other sialic acid-containing carbohydrates present on the intact syncytium and on endovascular invasive cytotrophoblasts.<sup>6</sup> Sequestration of parasitized erythrocytes in the placenta can give rise to maternal malaria, a severe syndrome associated with low birth weight, prematurity, and chronic intervillitis. PfEMP1 is presented in knoblike protrusions that anchor PfEMP1 to the erythrocyte membrane skeleton.<sup>7</sup>

Although the molecular players involved in cytoadhesion of parasitized erythrocytes are being characterized in ever-greater detail, the underpinning biomechanical principles are only partly understood. Previous studies have phenotypically described the adhesion behavior on different surfaces, revealing that parasitized erythrocytes firmly attach to CD36 and CSA but roll over surfaces containing ICAM 1, P-selectin, and VCAM 1 at physiological wall shear stresses.<sup>8-11</sup> Thus, central questions regarding the biomechanical factors that control the dynamics, efficiency, and strength of adhesion are still pending. The literature discusses several factors, including receptor and ligand geometry, bond characteristics, cell deformability, and the area of tight contact between the cell and the surface, that might affect the cytoadhesion of parasitized erythrocytes,<sup>12-15</sup> but their individual or combined contribution has not yet been experimentally specified.

Submitted March 6, 2014; accepted October 20, 2014. Prepublished online as *Blood* First Edition paper, October 28, 2014; DOI 10.1182/blood-2014-03-561019.

The online version of this article contains a data supplement.

There is an Inside *Blood* Commentary on this article in this issue.

The publication costs of this article were defrayed in part by page charge payment. Therefore, and solely to indicate this fact, this article is hereby marked "advertisement" in accordance with 18 USC section 1734.

© 2015 by The American Society of Hematology

Addressing these biomechanical factors has been hampered by the lack of amenable systems. For example, it is hardly feasible to quantitatively control the receptor arrangement on a microvascular endothelial cell or on stochastically receptor-coated plastic or glass surfaces. The advent of supported membranes (planar lipid bilayers deposited on solid substrates) that can be functionalized with adhesion receptors now enables us to address these defining biomechanical principles by allowing the distance between neighboring receptors to be controlled at nanometer accuracy.<sup>16,17</sup> Here, we have used functionalized membranes to study the biomechanics underpinning cytoadhesion of parasitized erythrocytes to CSA.

## Materials and methods

### *P. falciparum* strains and cultures

The *P. falciparum* strains FCR3 and FCR3<sup>Δvar2csa</sup> have been described previously.<sup>2</sup> Parasites were cultured as described and synchronized using the sorbitol method.<sup>18,19</sup> FCR3 was routinely selected by gelatin flotation and repeatedly panned over CSA-coated plastic dishes or CHO-K1 cells to obtain populations adhering to CSA.<sup>20,21</sup>

### Characterization of CSA

CSA (Sigma-Aldrich) was analyzed by 1-dimensional nuclear magnetic resonance spectroscopy. Seventy-seven percent of *N*-acetyl-D-galactosamines were sulfated at carbon C4, and 23% at carbon C6. The average molecular weight was 27.7 kDa, corresponding to a chain length of 60 disaccharide units, as determined by static light scattering (Zetasizer Nano ZS; Malvern).

### Preparation of supported membranes

The supported membranes were prepared as described previously.<sup>16</sup> Briefly, 1,2-dioleoyl-*sn*-glycero-3-phosphocholine (Avanti Polar Lipids) and 1,2-dioleoyl-*sn*-glycero-phosphoethanolamine-3-*N*-(cap biotinyl) (Avanti Polar Lipids) were solubilized in chloroform at molar ratios ranging from 0.02% to 5%. The lipid solutions were then dried under nitrogen flow and subsequently in a vacuum oven for 2 hours at room temperature. The dried lipids were resuspended in water and subsequently sonicated (0.5-second pulses for 30 minutes at 6 W with a Misonix 2000). Gas-permeable bottomless microfluidic chambers ( $\mu$ -Slide I, height 0.8 mm; ibidi) were sealed with RCA-cleaned glass slides (25 × 75 mm<sup>2</sup>; Menzel), using UV photobond (DELO). The vesicle suspension was filled into microfluidic chambers, where a lipid bilayer was formed by vesicle fusion on the glass slides. The chambers were rinsed with water and subsequently filled with an aqueous solution containing 5  $\mu$ g mL<sup>-1</sup> of neutravidin (Invitrogen) to saturate the biotin tags. CSA and other glycosaminoglycans (Sigma-Aldrich) were coupled with biotin, as described previously.<sup>22</sup> CSA was predominantly biotinylated at the carboxyl group of the terminal glucuronic acid, as determined by nuclear magnetic resonance. Biotinylated glycosaminoglycans at a concentration of 80  $\mu$ g mL<sup>-1</sup> in water were incubated with the neutravidin-saturated bilayers for 1 hour at room temperature. The functionalized membranes were subsequently washed with RPMI 1640 containing 11 mM glucose, 25 mM *N*-2-hydroxyethylpiperazine-*N'*-2-ethanesulfonic acid, and 2 mM glutamine (pH 7.6 at 37°C) (Gibco) and stored at 37°C. The intermolecular distance between CSA molecules was verified using quartz crystal microbalance with dissipation.<sup>23</sup>

### Cell adhesion experiments

Infected erythrocytes at the appropriate developmental stage were magnet purified (Miltenyi Biotec), yielding parasitemias of >90%.<sup>24</sup> Purified infected erythrocytes were resuspended in prewarmed complete RPMI 1640 medium at a concentration of 4 × 10<sup>7</sup> mL<sup>-1</sup>, as determined using a Z1 Coulter Particle Counter (Beckman Coulter). A 180- $\mu$ L cell suspension was injected into the microfluidic chamber. The filled chamber was incubated at 37°C for

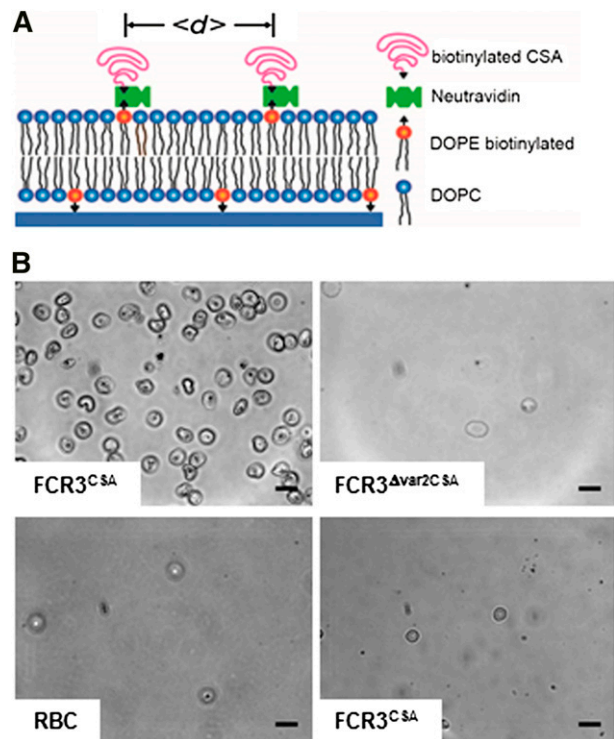


**Figure 1. Design and specificity of CSA-functionalized membranes.** (A) Schematic representation of the CSA-functionalized supported membrane. Components and the average distance between CSA molecules ( $\langle d \rangle$ ) are indicated. In the absence of an energetic favor, the CSA molecules assume a mushroom configuration. (B) Phase contrast images of functionalized membranes with 6-nm CSA spacing intervals reveal specific cytoadhesion of erythrocytes infected with FCR3<sup>Δvar2csa</sup> (upper left panel), and not of erythrocytes infected with FCR3<sup>CSA</sup> (upper right panel) or uninfected erythrocytes (RBC; lower left panel). FCR3<sup>CSA</sup> does not cytoadhere to nonfunctionalized membranes (lower right panel). Cells (4 × 10<sup>7</sup> mL<sup>-1</sup>) were allowed to settle on the membranes for 60 minutes under controlled atmospheric conditions before unattached cells were washed out at a wall shear stress of 0.8 Pa. Scale bar, 10  $\mu$ m. The images were taken using a digital camera (ORCA-ER charge-coupled device camera with Hokawo imaging software; Hamamatsu Photonics) mounted on a light microscope (Axiovert 200; Zeiss), original magnification ×63 (objective LD Achroplan 63x/0.75 corr. Ph2; Zeiss).

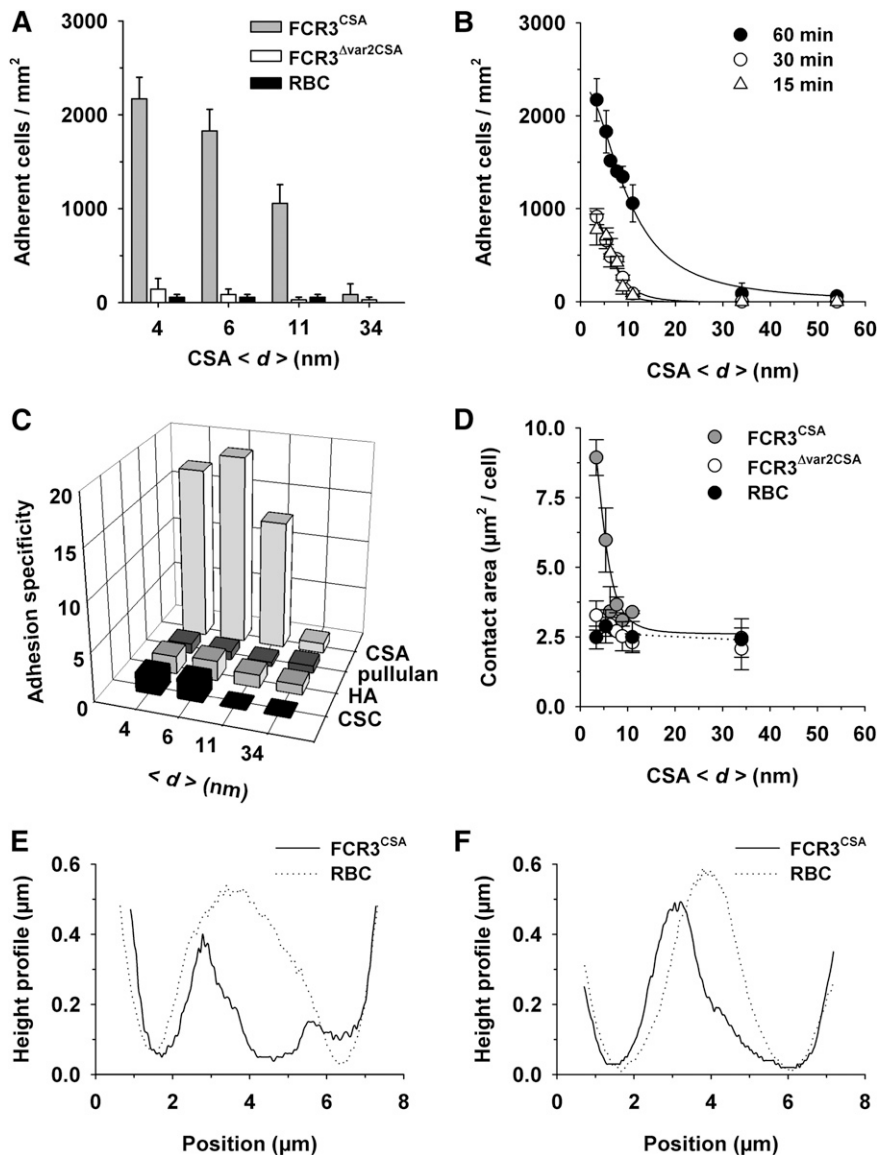
the time period indicated and kept in a moisture-saturated gas flow composed of 90% nitrogen, 5% oxygen, and 5% carbon dioxide during the course of the experiment. Unbound cells were washed out using a constant flow of medium at a wall shear stress of 0.8 Pa. Phase contrast images were collected using an Axiovert 200 microscope (Zeiss, Germany) equipped with an ORCA-ER charge-coupled device camera (Hamamatsu Photonics, Japan), and the number of adherent cells was counted. The same samples were subsequently reanalyzed by reflection interference contrast microscopy to determine the area of tight contact between the cell and the supported membrane.<sup>25</sup>

For adhesion assays under flow conditions, gas-permeable microfluidic chambers ( $\mu$ -Slide IV, height 0.1 mm; ibidi) were used. Purified infected erythrocytes (5 × 10<sup>6</sup>) at a concentration of 1 × 10<sup>6</sup> mL<sup>-1</sup> were flushed through the chamber at wall shear stresses ranging from 0.1 to 5 Pa before unbound cells were washed out using 5 mL of RPMI 1640 medium at the corresponding hydrodynamic condition. Adhesion assays in the presence of Duffy-binding-like (DBL) domain-specific antibodies (1:40 dilution) were performed as described previously.<sup>26</sup> Antibodies were preincubated with uninfected erythrocytes prior to the adhesion assay.

### Reconstruction of height profiles

Three-dimensional shapes of adherent cells near the membrane surface were reconstructed from 150 image stacks collected by a spinning disk brightfield confocal microscope (Nikon, Japan). The images were analyzed by the

**Figure 2. Effect of the intermolecular CSA distance on cytoadhesion of *P falciparum*-infected erythrocytes.** (A) Cytoadhesion behavior of erythrocytes infected with FCR3<sup>CSA</sup> or FCR3<sup>Δvar2CSA</sup> (trophozoite stage) or of uninfected erythrocytes (RBC) on functionalized membranes with different CSA spacing intervals ( $\langle d \rangle$ ). In panels A-D,  $4 \times 10^7$  cells mL<sup>-1</sup> were allowed to settle on the membranes for 60 minutes under controlled atmospheric conditions before unattached cells were washed out at a wall shear stress of 0.8 Pa. The means  $\pm$  standard deviation (SD) of at least 5 biological replicates are shown. (B) Cytoadhesion behavior of erythrocytes infected with FCR3<sup>CSA</sup> as a function of the intermolecular CSA distance and the incubation time. The following intermolecular distances between CSA molecules were investigated: 4, 6, 7, 8, 9, 11, 13, 16, 17, 34, and 54 nm, with an SD of 0.6 nm for all CSA distances. The data points were fitted using hyperbolic decay functions with Hill coefficient. (C) Cytoadhesion specificity of erythrocytes infected with FCR3<sup>CSA</sup> versus erythrocytes infected with FCR3<sup>Δvar2CSA</sup> on supported membranes functionalized with pullulan or with the glycosaminoglycans CSA, hyaluronic acid (HA), or chondroitin sulfate C (CSC). (D) Area of tight contact between the functionalized membrane and the cells indicated as a function of the intermolecular CSA distance. Effect of CSA distance on cell deformation is shown in the reconstructed 3-dimensional height profiles of the bottom planes of a single erythrocyte infected with FCR3<sup>CSA</sup> or an uninfected erythrocyte (RBC) resting on functionalized membranes, with a CSA spacing of 6 nm (E) and 11 nm (F). Representative height profiles of at least 10 biological replicates are shown.



iterative restoration method,<sup>27</sup> and the reconstructed profiles were projected with z-coded stack analysis as 2-dimensional contour images.

### Cell-detachment experiments

The CSA-functionalized membranes were placed in open liquid chambers, to which  $5 \times 10^3$  cells were added. The chambers were incubated for 1 hour at 37°C at controlled atmospheric conditions (see above). Adherent cells were detached from the CSA-functionalized membranes by using ultrasonic pressure waves ranging from 0.3 to 5.6 MPa, with stepwise increases in increments of 0.3 MPa, generated by intensive picosecond laser pulses.<sup>28</sup>

### Atomic force microscopy

Atomic force microscopy on air-dried parasitized erythrocytes was performed under ambient conditions as described previously.<sup>29</sup> The erythrocytes were imaged ( $512 \times 512$  pixels) with a scanning probe microscope (NanoWizard 3; JPK Instruments), using NANOSENSORS PPP-NCLR cantilevers (force constant: 21–98 N m<sup>-1</sup>; resonance frequency: 146–236 kHz) with scan speeds of 0.1 to 1.0 Hz, depending on scan size (0.25–15 μm). All images were processed and analyzed using JPK Image Processing software.

### Light scattering in solution

The size distribution of the purified VAR2CSA ectodomain (250 μg mL<sup>-1</sup> in phosphate-buffered saline, pH 7.2) in the presence of CSA (130 and 320 μg mL<sup>-1</sup>) or absence of CSA was determined by dynamic light scattering (Zetasizer Nano ZS; Malvern).<sup>30</sup> The heterologous expression of VAR2CSA in baculovirus-infected insect cells and the purification of the protein have been described previously.<sup>31</sup>

### Statistics

Data were analyzed using the Student *t* test, analysis of variance, and the *F* test.

## Results

### CSA distance defines cytoadhesion efficiency

We initially examined the binding behavior of 3 different cell treatments on CSA-functionalized membranes (Figure 1A): (1)

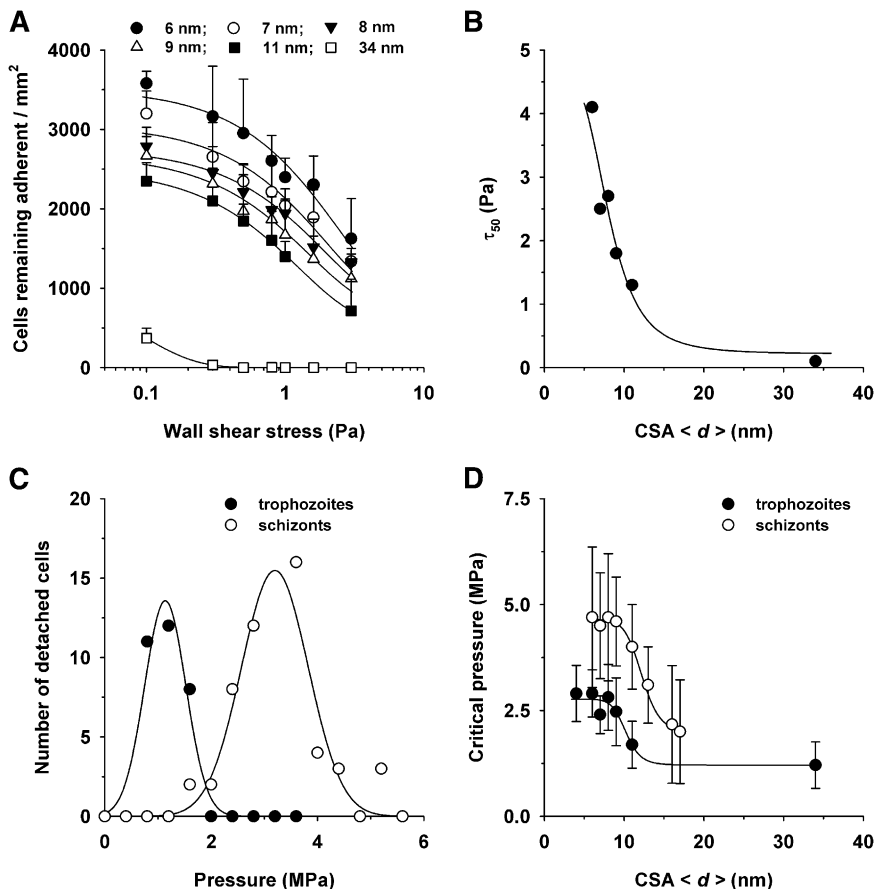


**Figure 3. Effect of the intermolecular CSA distance on the detachment of erythrocytes infected with FCR3<sup>CSA</sup>.** (A) Cells ( $4 \times 10^7 \text{ mL}^{-1}$ ) were allowed to settle on the CSA-functionalized membranes for 60 minutes under controlled atmospheric conditions before gradually increasing wall shear stresses (ranging from 0.1 to 5 Pa) were applied. The number of adherent cells were subsequently determined for each hydrodynamic condition and analyzed as a function of the wall shear stress. The mean  $\pm$  SD of at least 4 biological replicates are shown. The data points were fitted using an exponential decay function. (B) The wall shear stress at which 50% of the cells detached ( $\tau_{50}$ ) was determined for each hydrodynamic condition and analyzed as a function of the CSA distance. The data were fitted using a Hill function. (C) Erythrocytes infected with FCR3<sup>CSA</sup> at the trophozoite and schizont stages were allowed to adhere on a functionalized membrane with an intermolecular CSA distance of 6 nm for 60 minutes under controlled atmospheric conditions. Noncorpuscular ultrasonic pressure waves ranging from 0.3 to 5.6 MPa were applied, and the number of detachment events was observed as a function of the hydrodynamic pressure. (D) The critical pressures at which 95% of the adherent cells detached are shown as a function of the intermolecular CSA distance. The data points were fitted using a Hill function. The means  $\pm$  SD of at least 3 biological replicates are shown.

erythrocytes infected with the *P. falciparum* line FCR3 preselected for high-capacity binding to CSA (henceforth called FCR3<sup>CSA</sup>); (2) erythrocytes infected with the genetically engineered clone FCR3 <sup>$\Delta$ var2CSA</sup> in which the *var2csa* gene exclusively conferring cytoadhesion to CSA is disrupted and which consequently does not bind to CSA<sup>2</sup>; and (3) uninfected erythrocytes (adhesion to CSA-coated plastic dishes; see supplemental Figure 1 on the *Blood* Web site). Adhesion assays were performed using trophozoite-stage parasites (22–28 hours postinvasion). Cells were allowed to settle on the membranes ( $4 \times 10^7 \text{ mL}^{-1}$  cells per membrane) for variable time spans (15, 30, and 60 minutes) before unattached cells were washed out.

Uninfected erythrocytes and FCR3 <sup>$\Delta$ var2CSA</sup> did not bind to the CSA-functionalized membranes, whereas FCR3<sup>CSA</sup> bound in high numbers (Figure 1B). None of the cells adhered to nonfunctionalized membranes (Figure 1B). Quantification of the data confirmed the specific adhesion phenotype of FCR3<sup>CSA</sup>. Importantly, the adhesion efficiency strongly depended on the average molecular distance between CSA molecules, with the number of adherent cells rapidly declining as the CSA distance increased from 4 to 54 nm (Figure 2A–B). The number of adherent FCR3<sup>CSA</sup> further depended on the incubation time (Figure 2B), which we attribute to an increase in productive receptor/ligand interactions with time, facilitated by lateral diffusion. We fitted the data points by using a hyperbolic decay function with and without Hill coefficient. A Hill function was statistically favored in all cases, according to an F test (60 minutes:  $F = 16.8$ ,  $P < .009$ ; 30 minutes:  $F = 34.17$ ,  $P < .0007$ ; 15 minutes:  $F = 56.87$ ,  $P < .0002$ ). The Hill coefficients were  $-4 \pm 1$ ,  $-4 \pm 1$ , and  $-6 \pm 1$  for the 60-, 30-, and 15-minute data sets, respectively. We further obtained values for the intermolecular CSA distance that

produced half-maximal adhesion ( $d_{50}$ ). The  $d_{50}$  values of  $9 \pm 2 \text{ nm}$ ,  $7 \pm 2 \text{ nm}$ , and  $8 \pm 2 \text{ nm}$  for the 60-, 30-, and 15-minute data sets, respectively, were not statistically different from one another ( $P > .1$ ). Neither FCR3<sup>CSA</sup>, FCR3 <sup>$\Delta$ var2CSA</sup>, nor uninfected erythrocytes specifically bound to membranes functionalized with pullulan, chondroitin sulfate C, or hyaluronic acid (Figure 2C), consistent with previous studies.<sup>32</sup>

#### Contact area and cell deformation depend on CSA distance

The area of tight contact between parasitized erythrocytes infected with FCR3<sup>CSA</sup> and the supported membrane declined in a sigmoidal fashion with increasing CSA distance (Figure 2D). The Hill factor of  $-5 \pm 2$  and the  $d_{50}$  value of  $6 \pm 2 \text{ nm}$  were statistically not different from the values obtained in the adhesion assays. Three-dimensional-reconstructed confocal images revealed that the magnitude of the adhesion forces deformed the bottom planes of parasitized erythrocytes (Figure 2E–F), which explains the large contact area of  $9.0 \pm 0.6 \mu\text{m}^2$  observed on supported membranes with a CSA spacing of 6 nm.

In the case of FCR3 <sup>$\Delta$ var2CSA</sup> and uninfected erythrocytes, the contact area was independent of the CSA distance and remained constant at  $2.5 \pm 0.2 \mu\text{m}^2$  per cell (Figure 2D). Uninfected erythrocytes maintained their biconcave-discoid shape, indicating that they did not specifically interact with the CSA-functionalized membranes (Figure 2E–F).

#### Assessment of detachment forces

Previous studies have estimated the adhesion strength by exposing adherent parasitized erythrocytes to gradually increasing wall shear

stresses and by determining the pressure ( $\tau_{50}$ ) at which 50% of the cells detach.<sup>8</sup> For cytoadhesion to CSA, this value is approximately 1.3 Pa.<sup>11,33</sup> Our own wash-out experiments confirmed these studies and, in addition, showed that the CSA distance modulates the detachment process, resulting in a family of exponentially decaying curves (Figure 3A). The  $\tau_{50}$  values obtained from the curves correlated in an inverse sigmoidal fashion with increasing CSA distance (Hill factor of  $-11 \pm 2$  and a  $d_{50}$  value of  $12 \pm 2$  nm; Figure 3B).

We noted that many adherent cells were progressively deformed by the hydrodynamic pressure and eventually peeled off from the membrane. When a cell is peeled off from a surface, bonds gradually break, starting from the edge facing the pressure front. As a consequence, only relatively small pressures are required to detach a peeling cell. To obtain a more accurate estimation of the intrinsic adhesion strength, we explored an alternative detachment technique based on ultrasonic pressure waves induced by intensive picosecond laser pulses.<sup>28</sup> Because of the short contact time of approximately 80 ns, cells can engage only in elastic interactions without peeling effects.<sup>28,34</sup> Cells that were detached by this noninvasive and probe-free technique are fully viable and can readhere to surfaces.<sup>28</sup> Pressures in the lower MPa range were required to detach adherent parasitized erythrocytes infected with FCR3<sup>CSA</sup> from CSA-functionalized membranes. For example, at a CSA spacing of 6 nm, 95% of the cells were detached at a critical pressure of  $2.6 \pm 0.6$  MPa, as determined by analyzing the number of detachment events per pressure using a gaussian distribution (Figure 3C). The critical detachment pressure was determined for all CSA arrangements and analyzed as a function of the intermolecular CSA distance. A sigmoidal relationship emerged (Figure 3D), and fitting with a Hill function yielded a Hill factor of  $-11 \pm 3$  and a CSA  $d_{50}$  value of  $10 \pm 2$  nm.

In addition to trophozoites, we also investigated schizonts (32–40 hours postinvasion) to assess the effect of parasite maturation on the cytoadhesion strength. The resulting pressure diagram again revealed a sigmoidal relationship between the critical detachment pressure and the intermolecular CSA distance, but with a clear distinction. The critical pressure values were almost twice that determined for trophozoites for all CSA spacing intervals, whereas the curve parameters were largely maintained, including a Hill factor of  $-11 \pm 2.0$  and a  $d_{50}$  value of  $12 \pm 2$  nm. Apparently, developmentally controlled parasite factors affect the cytoadhesion strength of parasitized erythrocytes, in addition to the CSA arrangement.

One parasite factor might be the knobs, which serve as focal points for PfEMP1 presentation and whose surface density increases as the parasite matures.<sup>29,35</sup> To obtain quantitative data on knob number and distribution, we performed atomic force microscopy on erythrocytes infected with FCR3<sup>CSA</sup>. A significant increase in knob density from  $9 \pm 1$  to  $14 \pm 1 \mu\text{m}^{-2}$  ( $P = .02$ ) and a decrease in basal knob diameter from  $73 \pm 3$  to  $64 \pm 2$  nm ( $P = .004$ ) were observed as the parasite developed from trophozoites to schizonts (supplemental Figure 2A). The knob height remained constant ( $2.8 \pm 0.3$  nm; supplemental Figure 2B). Thus, the almost twofold increase in adhesion strength as the parasite develops from a trophozoite to a schizont cannot solely be correlated with the number of knobs. Additional contributing factors might be the developmental increase in surface-presented PfEMP1, membrane-bending rigidity, or both.<sup>36,37</sup>

### Shear-induced adhesion to CSA

We investigated how a variable receptor arrangement affects cytoadhesion of parasitized erythrocytes in laminar flow. We

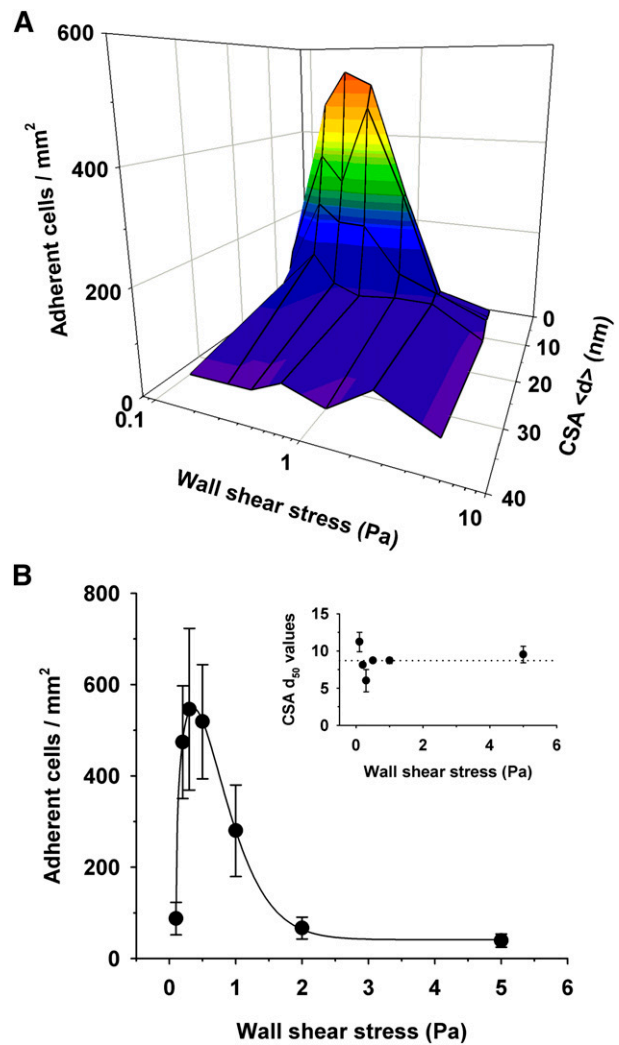


**Figure 4. Effect of the intermolecular CSA distance on adhesion of erythrocytes infected with FCR3<sup>CSA</sup> in flow.** (A) Parasitized erythrocytes at the trophozoite stage ( $1 \times 10^6$ ) were streamed through microfluidic chambers containing different CSA arrangements at the hydrodynamic conditions indicated. The number of adhering cells per square millimeter is shown as a function of the intermolecular CSA distance and the wall shear stress. (B) The number of cells adhering to a functionalized membrane with a CSA distance of 7 nm at different wall shear stresses. Inset: intermolecular CSA distance at which 50% of the cells adhere ( $d_{50}$ ) as a function of the wall shear stress. The  $d_{50}$  values were obtained by curve fitting the data points for each hydrodynamic condition. The means  $\pm$  SD of at least 3 biological replicates are shown.

perfused the CSA-supported membranes with cell suspensions at wall shear stresses ranging from 0.1 to 5 Pa, which covers the physiological range found in venular circulation (0.1 to 1.0 Pa, with transient peaks approaching 4.0 Pa).<sup>8,38</sup> The total number of parasitized erythrocytes streamed through the microfluidic chambers was constant for all hydrodynamic conditions ( $1 \times 10^6$ ). Cytoadhesion of parasitized erythrocytes was strongly dependent on the CSA distance under all hydrodynamic conditions and, in terms of the number of adherent cells, increased from none at a CSA distance of  $>34$  nm to efficient adhesion at a CSA distance  $<15$  nm (Figure 4A), thus replicating the findings made under static conditions. Curve-fitting each data set revealed comparable CSA  $d_{50}$  values for all wall shear stress conditions, with an averaged  $d_{50}$  value of  $9 \pm 1$  nm (Figure 4B). Furthermore, the cooperative nature of the interaction between VAR2CSA and CSA observed under static

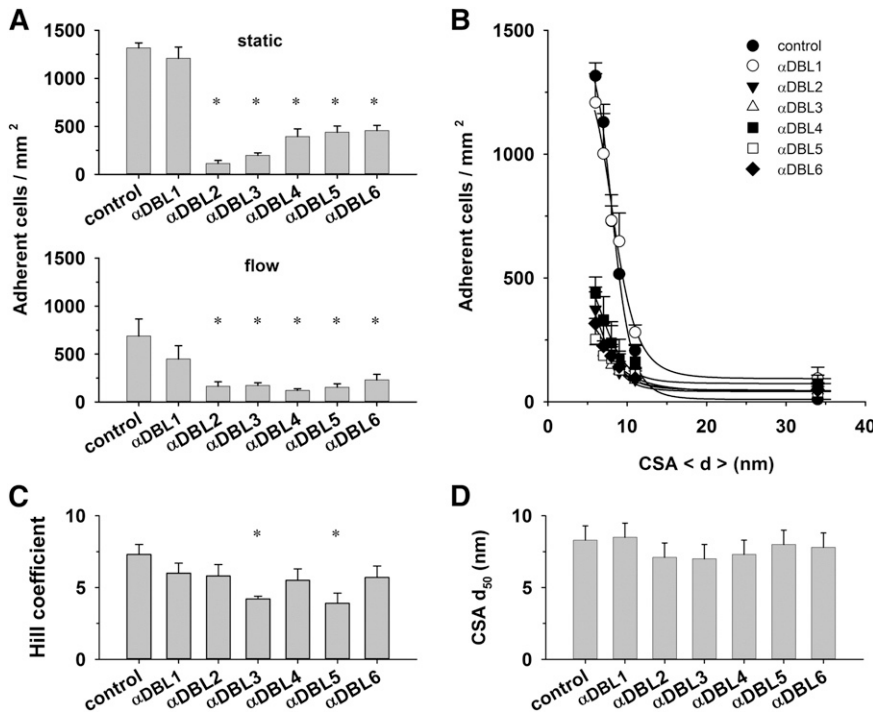


**Figure 5. Effect of DBL domain-specific antibodies on cytoadhesion.** (A) Erythrocytes ( $4 \times 10^7 \text{ mL}^{-1}$ ) infected with FCR3<sup>CSA</sup> were incubated with preadsorbed antibodies directed against the DBL domains indicated (dilution 1:40). Upper panel: cells were subsequently allowed to settle on CSA functionalized membranes (6-nm spacing) for 30 minutes before unbound cells were washed off and the number of adherent cells determined. Lower panel: the adhesion behavior was determined in laminar flow at a wall shear stress of 0.2 Pa. The means  $\pm$  SD of 4 biological replicates are shown. All assays were performed in parallel. (B) Number of adherent cells as a function of the CSA distance under static conditions. The curves presented in panel B were fitted using a Hill function, and the values for the Hill coefficient (C) and the CSA distance that supports half-maximal adhesion ( $d_{50}$ ) (D) were derived and analyzed as a function of the DBL domain-specific antibodies. \* $P < .01$ .

conditions also emerged in flow, with an average Hill coefficient of  $-5 \pm 2$ . Another feature revealed by the flow experiments was the pronounced dependence of the adhesion efficiency on tensile force, in that the number of adhering cells first increased and then decreased as the wall shear stress increased (Figure 4). Optimal adhesion occurred at a wall shear stress of  $0.2 \pm 0.1$  Pa for all CSA spacing intervals.

#### Antibodies against DBL domains affect cooperativity

Throughout the study, we noted cooperativity in the interaction of parasitized erythrocytes with CSA. One possibility to explain this result is that VAR2CSA can accept CSA at multiple cooperative binding sites. VAR2CSA harbors 6 DBL domains, several of which have been implicated in CSA binding, although no consensus has been reached as to whether all or only individual DBL domains interact with CSA.<sup>32,39-43</sup> To investigate the putative cooperative nature of the VAR2CSA/CSA interaction, we attempted to inhibit domain-specific regions of VAR2CSA using antibodies against the individual DBL domains.<sup>26</sup> We reasoned that these DBL domain-specific antibodies might interfere with substrate-induced allosteric changes and, thus, with the degree of cooperativity. The antibodies inhibited cytoadhesion to CSA under both static and flow conditions (Figure 5A-B).<sup>26,44,45</sup> Two of the 6 antibodies, namely those directed at DBL3X and DBL5ε, seemed to interfere with cooperative binding, indicated by significantly reduced Hill coefficients as determined in parallel assays (Figure 5C;  $P < .01$ ). The CSA  $d_{50}$  values were unaffected by the DBL domain-specific antibodies (Figure 5D).

We finally assessed the size distribution profile of the VAR2CSA ectodomain in solution. The 300-kDa protein existed in monodispersed form (Figure 6). The determined hydrodynamic radius of 9 nm was in good agreement with the calculated radius of gyration of the monomeric protein of 7 to 10 nm (depending on whether a rodlike or globular conformation was assumed). In the presence of CSA, the hydrodynamic radius shifted to a lower value of 7 nm (Figure 6), possibly because of conformational changes induced by the

binding of CSA. A minor population with a hydrodynamic radius of 15 nm also emerged, likely corresponding to CSA-cross-linked ectodomains.

## Discussion

CSA is present throughout the microvasculature, including the circulatory system of the lung and brain.<sup>46</sup> Yet it is only in the placenta that the parasite *P. falciparum* adheres to CSA in a process that involves specific expression of the distinct VAR2CSA adhesion molecule.<sup>2,4</sup> This contradiction might be explained by heterogeneity in CSA populations, with only the placental intervillous space harboring the low-sulfated CSA chains of at least 6 disaccharide repeats that support adhesion of *P. falciparum*-infected erythrocytes.<sup>3</sup> Our data provide an additional explanation, in that parasitized erythrocytes adhere to CSA only when the average distance between neighboring sugar chains is less than 15 nm, corresponding to a minimal density of 4400 CSA molecules per square micrometer. Although the precise CSA concentration in the placental intervillous space is unknown, one can assume it to be high. CSA can be extracted in substantial quantities ( $>100$  mg) from a single placenta, and electron microscopic studies revealed an amorphous electron-dense material in the intervillous space that was later identified as a CSA-containing proteoglycan matrix.<sup>47</sup> In comparison, the CSA content on the vascular endothelium is low. CSA is predominantly attached to thrombomodulin, a transmembrane protein involved in anticoagulation.<sup>46</sup> There are an estimated 50 000 to 100 000 thrombomodulin molecules on the luminal surface of an endothelial cell, of which only 10% to 20% are modified by a single CSA moiety.<sup>46</sup> Assuming a luminal surface of a vascular endothelial cell between 70 and 250  $\mu\text{m}^2$  and a random surface distribution of the thrombomodulin molecules,<sup>48</sup> this would amount to 20 to 200 CSA chains per square micrometer. These values are 1 to 2 orders of magnitude

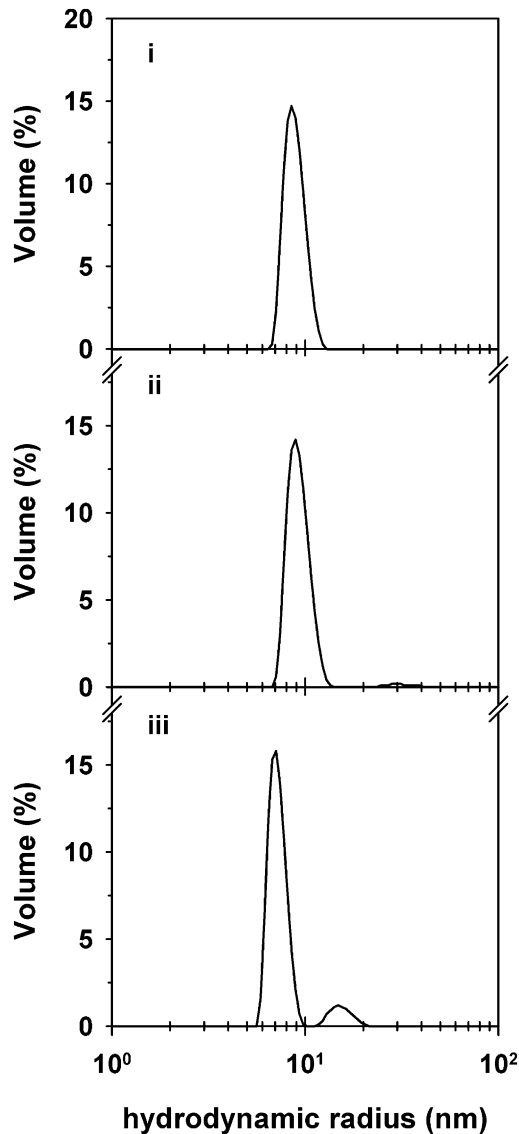


**Figure 6. Size distribution profile of the VAR2CSA ectodomain in the presence and absence of CSA in solution.** The size distribution by volume of purified VAR2CSA ectodomain ( $250 \mu\text{g mL}^{-1}$ ) in the absence (i) and in the presence of  $130 \mu\text{g/mL}$  CSA (ii) or  $320 \mu\text{g mL}^{-1}$  CSA (iii). Note the shift in the hydrodynamic radius of the VAR2CSA ectodomain in the presence of CSA and the appearance of a minor population with a hydrodynamic radius twice that of the major population. CSA is not detectable at the concentrations employed in this study. A representative example of 3 biological replicates is shown.

lower than the minimal CSA density required for adhesion of *P falciparum*-infected erythrocytes.

Discrimination between different CSA milieus is further aided by the cooperative nature of the CSA/VAR2CSA interaction. Cooperativity occurs when a protein has multiple ligand binding sites that exert an allosteric effect on one another such that binding of one ligand enhances or decreases the affinity for another ligand.<sup>49</sup> Cooperativity can also be found in oligomeric proteins, hemoglobin being the best-studied example.<sup>49</sup> The model of VAR2CSA being an oligomeric protein seems unlikely based on the size distribution profile of the purified VAR2CSA ectodomain, which predominantly existed as a monomer in solution (Figure 6). More in accord with the data is the model of VAR2CSA having multiple, cooperative CSA binding sites.

The ectodomain of VAR2CSA is 300 kDa in size and consists of 6 DBL domains (3 DBL domains each of the X and  $\epsilon$  classes), a cysteine-rich interdomain region between the second and third DBL domain, and short interspersed interdomain regions. The full-length ectodomain and a subfragment containing DBL2X plus flanking sequences bind CSA with high affinity *in vitro*.<sup>32,39,40</sup> In addition, x-ray crystallography has suggested an interaction of CSA with the DBLX3 and the DBL6 $\epsilon$  domains,<sup>41-43</sup> although some studies have questioned the selectivity and specificity of these DBL domains for CSA. However, these latter conclusions need to be revisited in light of our findings. If VAR2CSA is an allosteric protein, then one would expect single binding sites to have a low, if any, affinity for CSA when studied in isolation because the conformational changes through which different binding sites influence each other can take effect only in the native protein, and not in isolated binding domains. A mean Hill coefficient of  $5 \pm 2$  suggests that most, if not all, DBL domains of VAR2CSA form binding sites for CSA. Consistent with this model, antibodies directed against DBL3X and DBL5 $\epsilon$  significantly reduced the degree of cooperativity.

Adhesion of parasitized erythrocytes to CSA displays an interesting phenotype under variable hydrodynamic conditions, in that the amount of adhering cells first increases and then decreases as the wall shear stress is increased. Shear-enhanced adhesion is well-recognized in other systems, including FimH-mediated adhesion of *Escherichia coli* bacteria and selectin-mediated adhesion of leukocytes, and is explained by catch bonds—receptor/ligand interactions that are strengthened by tensile force owing to force-induced allosteric effects that prolong the half-life of the interaction.<sup>50,51</sup> On the basis of our hydrodynamic experiments, we propose that the interaction between VAR2CSA and CSA behaves like a catch bond when stressed. Shear-enhanced adhesion was also noted for rolling adhesion of parasitized erythrocytes to ICAM-1,<sup>8,10</sup> suggesting that it might be a feature common to different PfEMP1/receptor interactions. The wall shear stresses of 0.2 to 0.8 Pa that afforded adhesion to CSA correspond well with hydrodynamic conditions allegedly present in the intervillous space.<sup>52,53</sup>

Wash-out assays have been widely used to assess the adhesion strength of parasitized erythrocytes to CSA and other host receptors.<sup>8,11,33</sup> Although such assays mimic physiological hydrodynamic conditions, they grossly underestimate the intrinsic strength of the cell/receptor interaction. When adherent cells are exposed to increasing wall shear stresses, they deform under the hydrodynamic pressure and eventually peel off as bond after bond breaks. Removing adherent cells from a surface by using a micropipette or the cantilever of an atomic force microscope results in similar effects.<sup>8,13,54</sup> In comparison, ultrasonic pressure waves do not permit peeling effects or cell deformation. Because the noncorpuscular waves propagate at an ultrasonic speed of approximately  $1640 \text{ m s}^{-1}$ , the contact time is extremely short (approximately 80 ns), thereby limiting the effect on the cell to elastic interactions.<sup>34</sup> Thus, for the cell to detach from the contacting surface, all bonds need to rupture instantaneously and simultaneously. Consequently, pressures much higher than those used in wash-out assays are needed to detach cells. Further, the high loading rates applied in the laser ablation assay result in stronger interactions between noncovalent ligand/receptor pairs and, hence, higher unbinding forces.<sup>55</sup>

The detachment of parasitized erythrocytes from CSA is highly cooperative in a manner reminiscent of subunit cooperativity as is observed, for example, when a DNA helix melts. This finding suggests that the periodic pattern in which the CSA molecules are

presented on the supported membrane is matched by a similar periodic organization of the VAR2CSA molecules, suggesting that VAR2CSA, and possibly other PfEMP1 variants, are presented on the knobs in a defined geometric arrangement. In summary, our data suggest that the intermolecular CSA distance, the cooperative nature of VAR2CSA/CSA interaction, and the shear-enhanced binding behavior are defining parameters for the specific and selective cytoadhesion of *P falciparum*-infected erythrocytes in the placental intervillous space.

## Acknowledgments

The authors thank Stefan Prior for technical assistance. M.T. and M.L. are members of the German Excellence Cluster “CellNetwork.” M.T. and M.L. are further members of the Helmholtz Program “BioInterface” and the European Network of Excellence “EviMalR,” respectively.

This work was supported by the Deutsche Forschungsgemeinschaft under the Sonderforschungsbereich 1129 and the European Community’s Seventh Framework program grant “PreMalStruct.” The Institute for Integrated Cell-Material Science is supported by the

World Premier International Research Center Initiative, Ministry of Education, Culture, Sports, Science, and Technology, Japan. M.T. and H.Y.Y. thank the Japan Society for the Promotion of Science for the support by Kakenhi (grants 26247070 and 24680050) and the Brain Circulation Program, respectively.

## Authorship

Contribution: M.L. and M.T. conceived the study, analyzed the data, and wrote the manuscript; H.R., H.Y.Y., K.Q., M.A.N., C.P.S., and A.S. performed the experiments and analyzed the data.

Conflict-of-interest disclosure: The authors declare no competing financial interests.

Correspondence: Michael Lanzer, Department of Infectious Diseases, Parasitology, Heidelberg University, Im Neuenheimer Feld 324, 69120 Heidelberg, Germany; email: Michael.Lanzer@med.uni-heidelberg.de; and, Motomu Tanaka, Institute of Physical Chemistry, Physical Chemistry of Biosystems, Heidelberg University, Im Neuenheimer Feld 229, 69120 Heidelberg, Germany; email: tanaka@uni-heidelberg.de.

## References

1. Tembo D, Montgomery J. Var gene expression and human Plasmodium pathogenesis. *Future Microbiol.* 2010;5(5):801-815.
2. Viebig NK, Gamain B, Scheidig C, et al. A single member of the *Plasmodium falciparum* var multigene family determines cytoadhesion to the placental receptor chondroitin sulphate A. *EMBO Rep.* 2005;6(8):775-781.
3. Goel S, Gowda DC. How specific is *Plasmodium falciparum* adherence to chondroitin 4-sulfate? *Trends Parasitol.* 2011;27(9):375-381.
4. Salanti A, Staalsoe T, Lavstsen T, et al. Selective upregulation of a single distinctly structured var gene in chondroitin sulphate A-adhering *Plasmodium falciparum* involved in pregnancy-associated malaria. *Mol Microbiol.* 2003;49(1):179-191.
5. Fried M, Duffy PE. Adherence of *Plasmodium falciparum* to chondroitin sulfate A in the human placenta. *Science.* 1996;272(5267):1502-1504.
6. Hromatka BS, Ngeleza S, Adibi JJ, Niles RK, Tshetu AK, Fisher SJ. Histopathologies, immunolocalization, and a glycan binding screen provide insights into *Plasmodium falciparum* interactions with the human placenta. *Biol Reprod.* 2013;88(6):154.
7. Oh SS, Voigt S, Fisher D, et al. *Plasmodium falciparum* erythrocyte membrane protein 1 is anchored to the actin-spectrin junction and knob-associated histidine-rich protein in the erythrocyte skeleton. *Mol Biochem Parasitol.* 2000;108(2):237-247.
8. Nash GB, Cooke BM, Marsh K, Berendt A, Newbold C, Stuart J. Rheological analysis of the adhesive interactions of red blood cells parasitized by *Plasmodium falciparum*. *Blood.* 1992;79(3):798-807.
9. Cooke BM, Berendt AR, Craig AG, MacGregor J, Newbold CI, Nash GB. Rolling and stationary cytoadhesion of red blood cells parasitized by *Plasmodium falciparum*: separate roles for ICAM-1, CD36 and thrombospondin. *Br J Haematol.* 1994;87(1):162-170.
10. Yipp BG, Anand S, Schollaardt T, Patel KD, Looareesuwan S, Ho M. Synergism of multiple adhesion molecules in mediating cytoadherence of *Plasmodium falciparum*-infected erythrocytes to microvascular endothelial cells under flow. *Blood.* 2000;96(6):2292-2298.
11. Cooke BM, Rogerson SJ, Brown GV, Coppel RL. Adhesion of malaria-infected red blood cells to chondroitin sulfate A under flow conditions. *Blood.* 1996;88(10):4040-4044.
12. Korn C, Schwarz US. Efficiency of initiating cell adhesion in hydrodynamic flow. *Phys Rev Lett.* 2006;97(13):138103.
13. Li A, Lim TS, Shi H, et al. Molecular mechanistic insights into the endothelial receptor mediated cytoadherence of *Plasmodium falciparum*-infected erythrocytes. *PLoS ONE.* 2011;6(3):e16929.
14. Xu X, Efremov AK, Li A, et al. Probing the cytoadherence of malaria infected red blood cells under flow. *PLoS ONE.* 2013;8(5):e64763.
15. Fedosov DA, Caswell B, Suresh S, Karniadakis GE. Quantifying the biophysical characteristics of *Plasmodium-falciparum*-parasitized red blood cells in microcirculation. *Proc Natl Acad Sci USA.* 2011;108(1):35-39.
16. Tamm LK, McConnell HM. Supported phospholipid bilayers. *Biophys J.* 1985;47(1):105-113.
17. Tanaka M, Sackmann E. Polymer-supported membranes as models of the cell surface. *Nature.* 2005;437(7059):656-663.
18. Trager W, Jensen JB. Human malaria parasites in continuous culture. *Science.* 1976;193(4254):673-675.
19. Lambros C, Vanderberg JP. Synchronization of *Plasmodium falciparum* erythrocytic stages in culture. *J Parasitol.* 1979;65(3):418-420.
20. Jensen JB. Concentration from continuous culture of erythrocytes infected with trophozoites and schizonts of *Plasmodium falciparum*. *Am J Trop Med Hyg.* 1978;27(6):1274-1276.
21. Scherf A, Hernandez-Rivas R, Buffet P, et al. Antigenic variation in malaria: in situ switching, relaxed and mutually exclusive transcription of var genes during intra-erythrocytic development in *Plasmodium falciparum*. *EMBO J.* 1998;17(18):5418-5426.
22. Buffet PA, Gamain B, Scheidig C, et al. *Plasmodium falciparum* domain mediating adhesion to chondroitin sulfate A: a receptor for human placental infection. *Proc Natl Acad Sci USA.* 1999;96(22):12743-12748.
23. Rodahl M, Höök F, Kasemo B. QCM operation in liquids: an explanation of measured variations in frequency and Q factor with liquid conductivity. *Anal Chem.* 1996;68(13):2219-2227.
24. Ribaut C, Berry A, Chevalley S, et al. Concentration and purification by magnetic separation of the erythrocytic stages of all human Plasmodium species. *Malar J.* 2008;7:45.
25. Rädler J, Sackmann E. Imaging optical thicknesses and separation distances of phospholipid vesicles at solid surfaces. *J Phys II (France).* 1993;3(1):727-748.
26. Nielsen MA, Pinto VV, Resende M, et al. Induction of adhesion-inhibitory antibodies against placental *Plasmodium falciparum* parasites by using single domains of VAR2CSA. *Infect Immun.* 2009;77(6):2482-2487.
27. Gibson SF, Lanni F. Experimental test of an analytical model of aberration in an oil-immersion objective lens used in three-dimensional light microscopy. *J Opt Soc Am A.* 1992;9(1):154-166.
28. Yoshikawa HY, Rossetti FF, Kaufmann S, et al. Quantitative evaluation of mechanosensing of cells on dynamically tunable hydrogels. *J Am Chem Soc.* 2011;133(5):1367-1374.
29. Quadt KA, Barfod L, Andersen D, et al. The density of knobs on *Plasmodium falciparum*-infected erythrocytes depends on developmental age and varies among isolates. *PLoS ONE.* 2012;7(9):e45658.
30. Jachimiska B, Wasilewska M, Adamczyk Z. Characterization of globular protein solutions by dynamic light scattering, electrophoretic mobility, and viscosity measurements. *Langmuir.* 2008;24(13):6866-6872.
31. Dahlbäck M, Jørgensen LM, Nielsen MA, et al. The chondroitin sulfate A-binding site of the VAR2CSA protein involves multiple N-terminal domains. *J Biol Chem.* 2011;286(18):15908-15917.
32. Srivastava A, Gangnard S, Round A, et al. Full-length extracellular region of the var2CSA variant of PfEMP1 is required for specific,

- high-affinity binding to CSA. *Proc Natl Acad Sci USA*. 2010;107(11):4884-4889.
33. Avril M, Traoré B, Costa FT, Lépolard C, Gysin J. Placenta cryosections for study of the adhesion of *Plasmodium falciparum*-infected erythrocytes to chondroitin sulfate A in flow conditions. *Microbes Infect*. 2004;6(3):249-255.
  34. Engelhardt H, Sackmann E. On the measurement of shear elastic moduli and viscosities of erythrocyte plasma membranes by transient deformation in high frequency electric fields. *Biophys J*. 1988;54(3):495-508.
  35. Gruenberg J, Allred DR, Sherman IW. Scanning electron microscope-analysis of the protrusions (knobs) present on the surface of *Plasmodium falciparum*-infected erythrocytes. *J Cell Biol*. 1983;97(3):795-802.
  36. Kriek N, Tilley L, Horrocks P, et al. Characterization of the pathway for transport of the cytoadherence-mediating protein, PfEMP1, to the host cell surface in malaria parasite-infected erythrocytes. *Mol Microbiol*. 2003;50(4):1215-1227.
  37. Seifert U, Lipowsky R. Adhesion of vesicles. *Phys Rev A*. 1990;42(8):4768-4771.
  38. Papaioannou TG, Stefanadis C. Vascular wall shear stress: basic principles and methods. *Hellenic J Cardiol*. 2005;46(1):9-15.
  39. Clausen TM, Christoffersen S, Dahlbäck M, et al. Structural and functional insight into how the *Plasmodium falciparum* VAR2CSA protein mediates binding to chondroitin sulfate A in placental malaria. *J Biol Chem*. 2012;287(28):23332-23345.
  40. Srivastava A, Gangnard S, Dechavanne S, et al. Var2CSA minimal CSA binding region is located within the N-terminal region. *PLoS ONE*. 2011;6(5):e20270.
  41. Singh K, Gittis AG, Nguyen P, Gowda DC, Miller LH, Garboczi DN. Structure of the DBL3x domain of pregnancy-associated malaria protein VAR2CSA complexed with chondroitin sulfate A. *Nat Struct Mol Biol*. 2008;15(9):932-938.
  42. Higgins MK. The structure of a chondroitin sulfate-binding domain important in placental malaria. *J Biol Chem*. 2008;283(32):21842-21846.
  43. Khunrae P, Philip JM, Bull DR, Higgins MK. Structural comparison of two CSPG-binding DBL domains from the VAR2CSA protein important in malaria during pregnancy. *J Mol Biol*. 2009;393(1):202-213.
  44. Obiakor H, Avril M, Macdonald NJ, et al. Identification of VAR2CSA domain-specific inhibitory antibodies of the *Plasmodium falciparum* erythrocyte membrane protein 1 using a novel flow cytometry assay. *Clin Vaccine Immunol*. 2013;20(3):433-442.
  45. Fernandez P, Petres S, Mécheri S, Gysin J, Scherf A. Strain-transcendent immune response to recombinant Var2CSA DBL5-*c* domain block *P. falciparum* adhesion to placenta-derived BeWo cells under flow conditions. *PLoS ONE*. 2010;5(9):e12558.
  46. Martin FA, Murphy RP, Cummins PM. Thrombomodulin and the vascular endothelium: insights into functional, regulatory, and therapeutic aspects. *Am J Physiol Heart Circ Physiol*. 2013;304(12):H1585-H1597.
  47. Achur RN, Valiyaveetil M, Alkhalil A, Ockenhouse CF, Gowda DC. Characterization of proteoglycans of human placenta and identification of unique chondroitin sulfate proteoglycans of the intervillous spaces that mediate the adherence of *Plasmodium falciparum*-infected erythrocytes to the placenta. *J Biol Chem*. 2000;275(51):40344-40356.
  48. Garipcan B, Maenz S, Pham T, et al. Image analysis of endothelial microstructure and endothelial cell dimensions of human arteries – a preliminary study. *Adv Eng Mater*. 2011;13(1-2):B54-B57.
  49. Cui Q, Karplus M. Allostery and cooperativity revisited. *Protein Sci*. 2008;17(8):1295-1307.
  50. Le Trong I, Aprikian P, Kidd BA, et al. Structural basis for mechanical force regulation of the adhesin FimH via finger trap-like beta sheet twisting. *Cell*. 2010;141(4):645-655.
  51. Thomas WE. Mechanochemistry of receptor-ligand bonds. *Curr Opin Struct Biol*. 2009;19(1):50-55.
  52. Lecarpentier E, Bhatt M, Fournier T, Barakat A, Tsatsaris V. Numerical simulations of blood flows in the human placenta: estimation of the wall shear stress exerted on the syncytiotrophoblast. *Placenta*. 2014;35(9):A105.
  53. Peeters LLH, Buchan PC. Blood viscosity in perinatology. In: Scarpelli EM, Cosmi EV, eds. *Reviews in Perinatal Medicine*. Vol. 6. New York, NY: Alan R. Liss; 1989:53-89.
  54. Davis SP, Amrein M, Gillrie MR, Lee K, Muruve DA, Ho M. *Plasmodium falciparum*-induced CD36 clustering rapidly strengthens cytoadherence via p130CAS-mediated actin cytoskeletal rearrangement. *FASEB J*. 2012;26(3):1119-1130.
  55. Merkel R, Nassoy P, Leung A, Ritchie K, Evans E. Energy landscapes of receptor-ligand bonds explored with dynamic force spectroscopy. *Nature*. 1999;397(6714):50-53.



# blood

2015 125: 383-391

doi:10.1182/blood-2014-03-561019 originally published  
online October 28, 2014

## **Cytoadhesion of *Plasmodium falciparum*-infected erythrocytes to chondroitin-4-sulfate is cooperative and shear enhanced**

Harden Rieger, Hiroshi Y. Yoshikawa, Katharina Quadt, Morten A. Nielsen, Cecilia P. Sanchez, Ali Salanti, Motomu Tanaka and Michael Lanzer

---

Updated information and services can be found at:

<http://www.bloodjournal.org/content/125/2/383.full.html>

Articles on similar topics can be found in the following Blood collections

[Free Research Articles](#) (3000 articles)

[Red Cells, Iron, and Erythropoiesis](#) (625 articles)

---

Information about reproducing this article in parts or in its entirety may be found online at:

[http://www.bloodjournal.org/site/misc/rights.xhtml#repub\\_requests](http://www.bloodjournal.org/site/misc/rights.xhtml#repub_requests)

Information about ordering reprints may be found online at:

<http://www.bloodjournal.org/site/misc/rights.xhtml#reprints>

Information about subscriptions and ASH membership may be found online at:

<http://www.bloodjournal.org/site/subscriptions/index.xhtml>